

# Contamination transport from spacecraft due to winds

Parthasarathy Shakkottai, Thermal and Fluids Systems Engineering, Jet Propulsion Laboratory, California Institute of Technology, 4800 Oak Grove Dr, Pasadena Ca 91109,

Julian Bunn , Caltech Center for Advanced Computing Research, California Institute of Technology, 1200 E California Blvd, Pasadena, Ca, 91125

and

Jackie Grimes, Student, 742 Cochran Street  
Sewickley PA 15143

*Abstract:* Particle transport from spacecraft surfaces to the ground due to Martian winds is of interest in estimating contamination levels. There are two aspects to the problem. First we have to find how particles detach from surfaces in a given wind and next determine particle trajectories and final landing points.

Particle detachment from surfaces occurs when the moment due to particle drag in the wall shear region overcomes the restraining moment due to adhesion and gravitational forces. Available experimental data are compared with theoretical expressions of adhesion moment based on areas of contact of smooth, rough, elastic and plastic deformations. It turns out that smooth elastic contact is best supported by experimental data.

Rules for determining local winds on a bluff body are given based on locating stagnation points and attached flow regions.

The last step is to solve for trajectories given an initial particle distribution which is distributed at random on various surfaces and allowed to be dislodged by a wind distribution. An example will be shown of result from the Contamination Transport Program developed in Java which takes as input a vrmf file of a lander and a cleanliness level and calculates particle trajectories and distributions on the ground.

## 1 INTRODUCTION

Particle transport from spacecraft surfaces to the ground due to Martian winds is of interest in estimating contamination levels. There are two aspects to the problem. First we have to find how particles detach from surfaces in a given wind and next determine particle trajectories and the final landing point.

Particle detachment from surfaces occurs when the moment due to particle drag in the wall shear region overcomes the restraining moment due to adhesion and gravitational forces. Available experimental data are compared with theoretical expressions of adhesion moment based on areas of contact of smooth, rough, elastic and plastic

deformations. It turns out that smooth elastic contact is best supported by experimental data.

Rules for determining local winds on a bluff body are given based on locating stagnation points and attached flow regions where shear stresses are present. In separated flow regions, there is practically no flow.

The last step is to solve for trajectories given an initial particle distribution which is distributed at random on various surfaces and allowed to be dislodged by a wind distribution. A Contamination Transport Program has been developed in Java which calculates trajectories. It takes as input a vml file of a lander and a particle size distribution specified by a cleanliness level, distributes the particles at random on all surfaces, subjects them to a specified wind profile and calculates particle trajectories and distributions on the ground.

### **Background:**

Most of the experimental data required for developing correlations comes from the thesis (available on the web) "*MICROPARTICLE DETACHMENT FROM SURFACES BY FLUID FLOW*" by Abdelmaged Hafez Ibrahim Essawey's Ph.D thesis, Notre Dame, Indiana, Jan 2004, pp1-139. Experimental data were obtained under careful conditions as described in his abstract which says "This work presents a combined experimental and theoretical investigation of the conditions under which a fluid flow causes a microparticle to detach from a flat surface. The general approach was to conduct well-controlled experiments, to observe individual

microparticle motion and to focus on the basic detachment mechanisms. Microparticles of different sizes, materials and shapes (mostly microspheres) were deposited as monolayers onto the substrates under controlled conditions. The microparticles attached to the substrate in a condition of static equilibrium due to contact adhesion and resided completely within the viscous sublayer.

The flow was accelerated during a transient period up to a fixed, constant velocity. Smooth glass plates were used as substrates and scanned with an atomic force microscope to determine their roughness-height distributions. The study was confined to microparticles in the diameter range of approximately 10  $\mu\text{m}$  to 100  $\mu\text{m}$ . They were distributed on the surface as a monolayer in sparse/dense conditions, dry/humid and subjected to laminar or fully developed turbulent flows. Quantitative information on the increase of flow velocity at which 50 % of the microparticles detached ( $U_{th}$ ) at different controlled conditions are presented. The variability in the  $U_{th}$  was found to be in the range of 10 % to 20 %. The techniques used to obtain such a low variability are described. The measured values then were compared to a model based on force/moment balance approach. The model accounts for the surface roughness effects and is applicable to dry/humid conditions and laminar or fully developed turbulent flows. The results of the model agreed with the measurements, to within the uncertainties, for the cases studied. The sensitivity of the  $U_{th}$  to five factors contained in the experiments and the model is analyzed. The motion of microparticles after their detachment is considered. The microparticle velocities along the surface after detachment are

measured using a strobed laserlight sheet and compared to the numerical solutions. Results indicate that the microparticles undergo pure rolling along the surface before possible entrainment, that the sweep part of a burst-sweep event plays a role in the detachment process and that the dissipative forces and moments are negligible.”

### Characteristics of particle detachment:

Particles of a uniform size are distributed on a flat surface at low surface number density and are subject to a wind which rises from zero to a specified velocity in a short time and then held at that value for a long time. During the process of rapid velocity change, a certain fraction of particles detach and during the period of constant wind particles continue to detach. Sketches in Figure 1 and Figure 2 show the ideal and practical nature of data. Specifically, Figure 2 shows a period of constant wind resulting in particle detachment. Essawey’s data is given in the form of detachment ratio vs. wind speed corresponding to the ideal behavior describing the prompt effect of the wind. For application on Mars, we use the data in the same form.

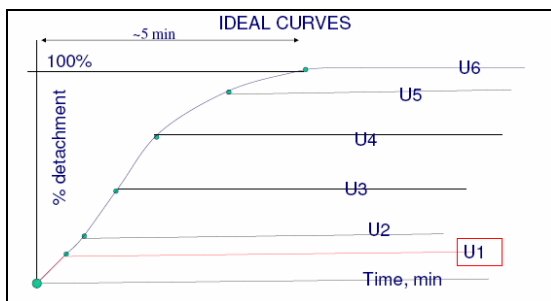


Figure1. The detachment fraction as a function of wind speed is shown here. If the wind speed increases to U6 from zero and

the undetached fraction is measured at times corresponding to velocities U1, U2...U6 by taking snapshots of particles present in the field of view, we get the data points shown as green circles. If the flow is held at a wind speed U3, ideally everything stays frozen and no more particles detach. If the wind speed is reduced to U2, again there is no detachment. Those particles that will detach do so as the wind speed is increasing. On the way back to zero there is no detachment.

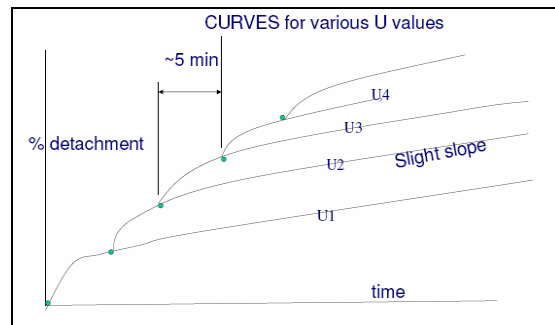


Figure 2. The result of a practical experiment (as compared to an ideal one in figure 1) is sketched above. If the wind speed is increased from 0 to U1, we see a region of quick detachment followed by a slow rise with a slope that is much lower. If the velocity U5 in the above plot is large enough to detach all particles in the initial period of rapid detachment, the slope in the slow period will be zero even in the non-ideal case because there are no more particles to detach.

## 2 FORMULATION OF THE PROBLEM

First we start from the forces and moments that are needed to dislodge a particle resting on a surface. Then we examine the nature of the predicted dislodgement function and compare the predictions to available data.

A good review of particle deformation is the reference “Physical Interactions affecting the adhesion of dry particles” by Rimai and DeMejo, Annual Rev.

Material Sci. 1996. 26:21-41, also available as Annual Reviews, [www.annualreviews.org/aronline](http://www.annualreviews.org/aronline). There are many expressions for the contact radius of a particle of radius R in contact with a flat surface which are described below. Also the equations needed to calculate the detachment fraction are given.

JKR (ref 1) and DMT (ref2) are two theories that explain adhesion of spheres to plane surfaces. We define terms and equations as we proceed. The interatomic distance is a quantity which is the scale for van Der Waal's forces. Typically,

$$z_0 = 4 \times 10^{-10} \text{ meters} \quad (1)$$

The van der Waals constant, called Hamaker's constant is given by

$A_1 = 8 \times 10^{-20}$  J as a sample value for polystyrene. The web site Clarkson University adhesion lists tables of A.  $A_1$  is related to surface energy equal to work done in forming a unit area by

$$W_A = \frac{A_1}{12 \times \pi \times z_0^2} \quad (2)$$

For the value of  $A_1$  given above,  $W_A = 0.0133 \text{ J/m}^2 = 13.3 \text{ dyne/cm}$ . The surface tension  $\gamma$  is the same as  $W_A$ .

The elastic moduli of the two materials combine in the form of a composite modulus

$$K_1 = \left( \frac{1 - \nu_1^2}{E_1} + \frac{1 - \nu_2^2}{E_2} \right)^{-1} \quad (3)$$

where 1 refers to the particle and 2 refers to the surface and E is the Young's

modulus and  $\nu$  is the Poisson's ratio.  $K_2 = 4/3 K_1$  in Rimai's review.

Sometimes this is defined with numerical factors such as  $4/3$  or  $4/3 \pi$  inserted to make some formulas appear simpler. It is best not to do this because it generally adds to confusion because the same symbols mean different things.

**JKR theory:** The restraining moment (holding moment) holding a particle of radius R is the product of the adhesion force

$$F_A = 1.5 \times \pi \times \gamma \times R, \text{ and the contact radius} \quad (4)$$

$$a_{JKR} = \left( \frac{6 \times \pi \times \gamma \times R^2}{K_2} \right)^{\frac{1}{3}} \quad (5)$$

from the JKR theory. The expression for the restraining moment is

$$Moment_{JKR} = \frac{3}{2} \times \pi \times \gamma \times R_1 \times \left( 6 \times \pi \times \gamma \times \frac{R_1^2}{K_2} \right)^{\frac{1}{3}} \quad (6)$$

**Derjaguin's theory:** His equation(from Rimai's Annual Review) is

$$a_{derja} = \left( \frac{9 \times \pi \times \gamma}{2} \times \frac{1 - \nu\nu^2}{E} \times R^2 \right)^{\frac{1}{3}} \quad (7)$$

where E is the Young's modulus and  $\nu\nu$  is the Poisson's ratio of the deforming material. This also varies as  $R^{\frac{2}{3}}$ . The moment becomes

$$Moment_{derja} = \frac{3}{2} \times \pi \times \gamma \times R_1 \times \left( \frac{9 \times \gamma}{8} \times \frac{1 - \nu\nu^2}{E} \times R^2 \right)^{\frac{1}{3}} \quad (8)$$

**Kendal's expression:** Johnson et.al showed that the contact radius is related to load applied by

$$a(W_1, R_1) = \left[ \frac{3}{4} \times \frac{1 - \nu\nu^2}{E} \times R_1 \times \left[ W_1 + (3 \times \pi \times R_1 \times \gamma) + \left[ (3 \times \pi \times R_1 \times \gamma)^2 + 6 \times \pi \times R_1 \times \gamma \times W_1 \right]^{\frac{1}{2}} \right] \right]^{\frac{1}{3}} \quad (9)$$

With  $W_1$  representing the downward load. If both materials deform, the term  $\frac{1 - \nu\nu^2}{E}$  is replaced by the composite value  $\frac{1}{K}$ . When  $W_1$  is zero, we get

$$a_0(R_1) = \left( \frac{9}{2} \times \pi \times \frac{1 - \nu\nu^2}{E} \times R_1^2 \times \gamma \right)^{\frac{1}{3}} \quad (10)$$

with  $a_0$  indicating no external load. This is the same as Kendall's expression. Kendall verified the correctness of this equations and the one for  $a(W_1, R_1)$  by experiments on large gelatin spheres of diameter equal to 2.5 cm, 7.9 cm and 25.5 cm.

**First principles:** Let us look at this in terms of the contact area which is a circle of radius  $a$ . If  $a$  is the radius of the contact patch, the holding moment is the product of moment arm  $a$  and the downward force equal to the area times adhesion stress (force per unit area). The moment arm is  $a$  and not  $2a$  because the lifting force is along the central axis and the sphere tips around a point on the circumference.

$$Holding\ Moment = a \times \pi \times a^2 \times stress$$

By definition, work done in producing a surface is related to  $A_1$  by

$$\frac{work}{area} = \frac{A_1}{12 \times \pi \times z_0^2} \quad (11)$$

where  $A_1$  is the Hamaker's constant. Using  $work\ done = force \times a \times z_0$  with  $\alpha$  on the order of 1, representing the range of van Der Waal's force,

$$\frac{force}{area} = \frac{a_1}{12 \times \pi \times z_0^2} \times \frac{1}{z_0 \times \alpha}, \text{ and the holding moment is given by} \quad (12)$$

$$Holding\ Moment = a \times \pi \times a^2 \times \frac{A_1}{12 \times \alpha \times \pi \times z_0^3} \quad (13)$$

$$Holding\ Moment(a) = \left( \frac{a}{z_0} \right)^3 \times \frac{A_1}{12 \times \alpha} \quad (14)$$

This is equal to the product  $F_A$  the pull-off force and moment arm  $a$  to get

$$\frac{3}{2} \times \pi \times \gamma \times R_1(a) = \left( \frac{a}{z_0} \right)^3 \times \frac{A_1}{12 \times \alpha} \quad (15)$$

and

$$a(R_1) = \left( \frac{12 \times \alpha}{A_1} \times \frac{3}{2} \times \pi \times \gamma \times R_1 \times z_0^3 \right)^{\frac{1}{2}} \quad (16)$$

This varies as the square root of  $R_1$ . Rimai shows examples of both  $\frac{1}{2}$  power and  $\frac{2}{3}$  power variations of contact radius with particle radius. The predicted values of  $a$  are plotted below in Figure 3 to show typical values.

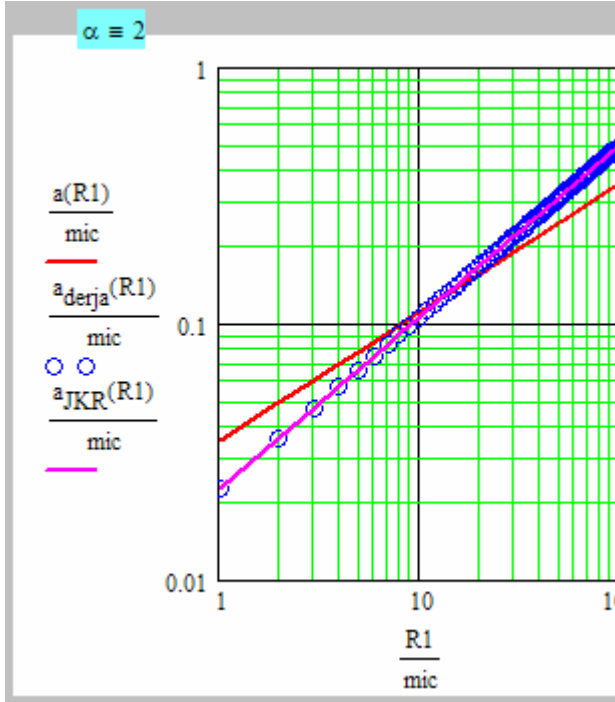


Figure 3. Variations of contact radius from JKR, from Derjaguin and from first principles are shown above. Material constants are for glass.  $\gamma$  is 13.3 dyne/cm.  $\rho$  has been set to 2. The contact radius from 0.05  $\mu$  to 0.1  $\mu$  at  $R = 10 \mu$ .. Deformation increases with  $\alpha$ .

**Moment ratios:** We are interested in ratios of moments due to aerodynamic drag compared to the restraining moments due to adhesion and gravity.

The moment due to weight is the product of the vertical force

$$\frac{4}{3} \times \pi \times R_1^3 \times \rho_p \times g$$

(17)

and the moment arm  $a$  given by various expressions.  $\rho_p$  is the density of the material of the particle,  $g$  is the gravitational acceleration and  $R_1$  is the particle radius. The aerodynamic drag of a particle present at the wall in the sublayer is the Stokes drag corresponding to  $velocity = \frac{\tau \times R}{\mu}$  in the linear profile region at a distance  $R$  from the wall. This is

$$6\pi\mu \times R_1 \times \frac{\tau \times R}{\mu}$$

(18)

$= 6\pi\mu \times R_1^2 \times \tau$ . A correction  $h = 1.7$  is applied to take account of a wall effect. The moment then becomes  $h R_1$  times the force.

$Drag\ moment = 6R_1^3 \times \tau \times h$ , for a particle of radius  $R_1$  and wall shear stress  $\tau$ . The ratio of moments is the function that represents the particle detachment function. Using Kendall's theory for  $a$ , we evaluate

$$F = \frac{\tau \times R_1^3 \times 6 \times \pi \times h}{a^2 \times surface\ tension + weight \times a}$$

(19)

which becomes the function  $F_5$  which depends on  $R_1$  and  $\tau$ .

$$F_5(R_1) = \frac{\tau \times R_1^3 \times 6 \times \pi \times h}{\gamma \times \left( \frac{3}{4} \times \frac{1 - \nu \nu^2}{E} \times R_1 \times 6 \times \pi \times R_1 \times \gamma \right)^{\frac{2}{3}} + \rho_p \times g \times \frac{4}{3} \times \pi \times R_1^3 \times \left( \frac{3}{4} \times \frac{1 - \nu \nu^2}{E} \times R_1 \times 6 \times \pi \times R_1 \times \gamma \right)^{\frac{1}{3}}}$$

(20)

Here, a is the term in square brackets with the 1/3 power and its square appears in the first term in the denominator. This term is the product of a force = a  $\gamma$  and moment arm a. This assumes that the force required to allow rolling is (a.  $\gamma$ ) instead of the pulloff force (3/2) ( $\gamma.R.\pi$ ) seen earlier. We will compare this and similar expressions to

available data and show that this result fits experiments best.

It is more convenient to plot results in the form of  $\tau$  vs. R1 with F as a parameter.

$$\tau_1(R_1, F_5) = \frac{F_5}{R_1^3 \times 6 \times \pi \times h} \left[ \gamma \times \left( \frac{3}{4} \times \frac{1 - \nu \nu^2}{E} \times R_1 \times 6 \times \pi \times R_1 \times \gamma \right)^{\frac{2}{3}} + \rho_p \times g \times \frac{4}{3} \times \pi \times R_1^3 \times \left( \frac{3}{4} \times \frac{1 - \nu \nu^2}{E} \times R_1 \times 6 \times \pi \times R_1 \times \gamma \right)^{\frac{1}{3}} \right]$$

(20)

It is best to illustrate the nature of this function by a set of curves with varying

F as shown in Figure 4. The curves are for glass particles on a glass surface under earth gravity.

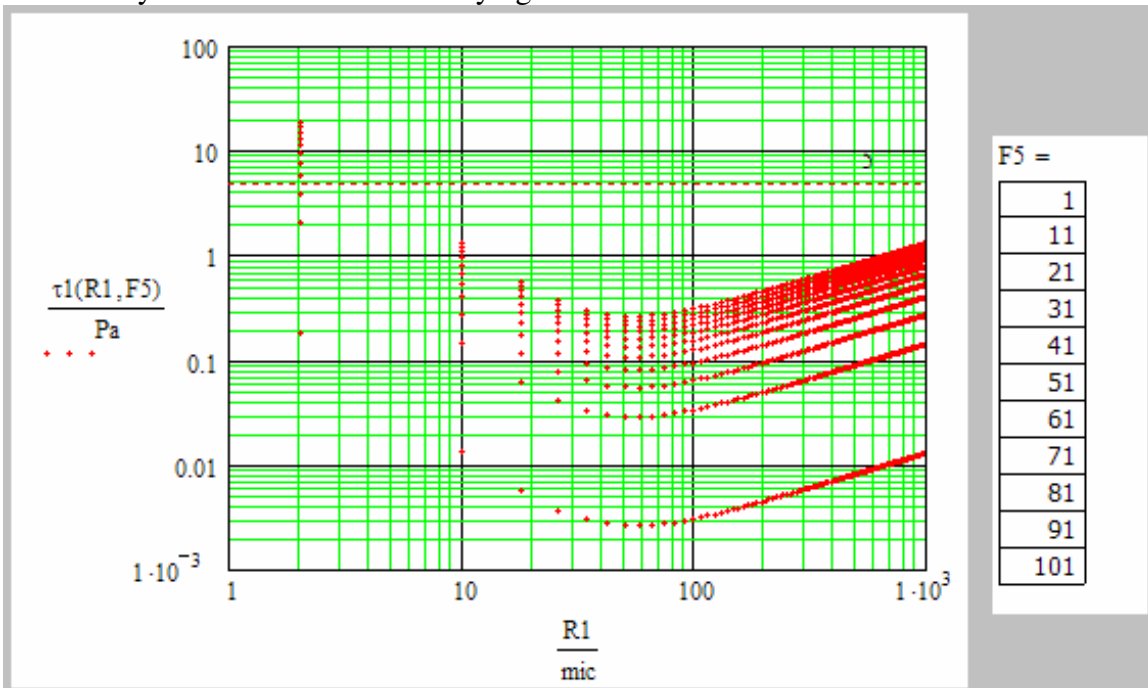


Figure 4. This plot shows how the wall stress (Pa) required to dislodge particles depends on R1 in  $\mu$ . It decreases with R1 until the gravity term becomes significant and later becomes dominant compared to adhesion. The lowest curve is for F5 equal

to 1, a value near incipient rolling and curves above this are for values 11, 21, ....101. Each curve represents a fixed % detachment equal to the value of F5. There is no rolling motion below the lowest curve and there are no particles left to be

dislodged above the topmost curve. The band occupied between the curves covers the region of particle detachment. The region near 50  $\mu$  is dislodged most easily and the shear stress required is  $\sim 0.01$  to  $0.1$  Pa.

### Other expressions:

The holding moment is determined by the assumptions made. For **rough surface contact** the moment arm is the mean distance between high points of the rough particle, rough surface or a combination of the two. This is the product of force  $\gamma.R_1$  and arm  $2.\alpha.z_0$  where  $\alpha$  is a number representing the range of action of van Der Waal's forces.

$$M_1 = \gamma \times R_1 \times 2 \times \alpha \times z_0. \quad (21)$$

The second is based on pull off force and  $a$  from JKR theory. This is written as

$$M_2 = 1.5 \times \gamma \times R_1 \times a. \quad (22)$$

The third is based on the smaller contact area and is calculated by perimeter times surface tension times the moment arm,  $a$ .

$$M_3 = 2 \times \pi \times a^2 \times \gamma. \quad (23)$$

The equations for functions F are as follows.

$$F_1(R_1) = \frac{\tau \times R_1^3 \times 6 \times \pi \times h}{\left(\frac{3}{2} \times \pi \times \gamma \times R_1 + \frac{4}{3} \times \pi \times R_1^3 \times \rho_p \times g\right) \left(6 \times \pi \times \gamma \times \frac{R_1^2}{K_2}\right)^{\frac{1}{3}}} \quad (24)$$

The denominator is the sum of adhesion and weight multiplied by the moment arm,  $a$ , as in (19).

For rough surface contact we get

$$F_1(R_1) = \frac{\tau \times R_1^3 \times 6 \times \pi \times h}{\left(\gamma \times \sqrt{2 \times \alpha \times R_1 \times z_0} + \frac{4}{3} \times \pi \times R_1^3 \times \rho_p \times g\right) \times N_1 \times z_0}. \quad (25)$$

Here the moment arm is replaced by  $N_1 z_0$ , the distance between two bumps.  $\alpha$  is a measure of the extent of the van der Waal force. The numerator is the aerodynamic rolling moment. The denominator is the moment due to restraining forces of adhesion and gravity with a moment arm equal to  $N_1 z_0$ .

The third equation is for smooth surface contact but with a smaller area of contact based on a force acting over a circle of radius  $a$ .

$$F_3(R_1) = \frac{\tau \times R_1^3 \times 6 \times \pi \times h}{\left[ 2 \times \pi \times \gamma \times \left( 6 \times \pi \times \gamma \times \frac{R_1^2}{K_2} \right)^{\frac{1}{3}} + \frac{4}{3} \times \pi \times R_1^3 \times \rho_p \times g \right] \left( 6 \times \pi \times \gamma \times \frac{R_1^2}{K_2} \right)^{\frac{1}{3}}} \quad (26)$$

The three expressions can be compared by plotting them in the form

$$\tau_1(R_1, F_1) = \frac{F_1}{R_1^3 \times 6 \times \pi \times h} \times \left( \frac{3}{2} \times \pi \times \gamma \times R_1 + \frac{4}{3} \times \pi \times R_1^3 \times \rho_p \times g \right) \times \left( 6 \times \pi \times \gamma \times \frac{R_1^2}{K_2} \right)^{\frac{1}{3}} \quad (27)$$

with similar expressions for the other two. The rough surface and smooth overlap at small particle sizes but are otherwise well separated from one another. The smooth surface theory with relationship between shear stress and particle radius in the presence of gravity is closest to experimental data to be described later. Figure 5 shows the

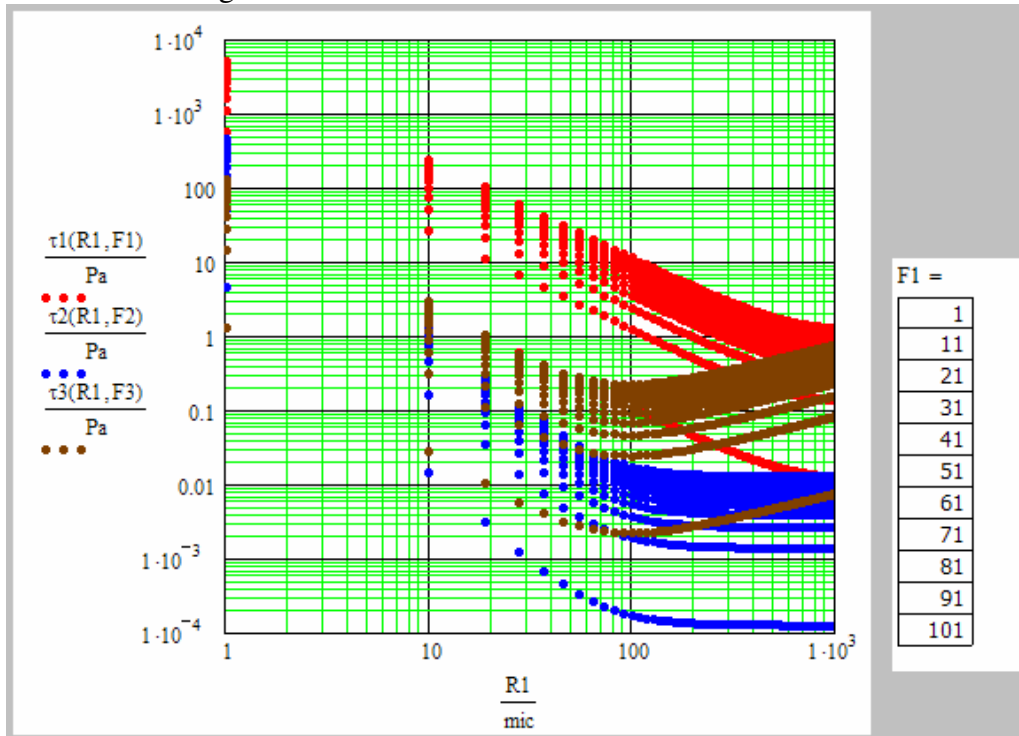


Figure 5. This is a plot of shear stress vs. particle radius under earth gravity. The red curves are based on the pulloff force (proportional to  $R_1$  and not  $a$ ) and require high values of shear stress for

dislodgement. The brown curves are for smooth surface contact with the area based on 'a' and the adhesion force also based on the area of contact. The shape of the brown curves resembles experimental data. The blue curves have a constant moment arm and dislodge easily at large sizes. As the size decreases, the curves rise more steeply

and overlap the smooth surface curves in the micron region. Roughness may be important in that region. The curves are all for glass on glass with  $N1=350$  and  $a = 100$  and density =  $3 \text{ gm/cm}^3$ .

## DATA FITS

Here we examine particle detachment data from Essawey's thesis and from other sources. Consider glass microspheres on a glass surface. Points were read from a curve plotting the detachment fraction vs. wind speed at low humidity. Below 30% relative humidity, the detachment curves are not dependent on humidity. The drag moment is given by the numerator of (19) with the wall shear stress given by

$$\tau := \left[ \frac{1}{2} \cdot \rho \cdot U^2 \cdot \frac{0.0583}{(\text{Re}_x + 0.001)^{0.2}} \right]$$

with the skin friction coefficient associated with a flat plate turbulent boundary layer,

$$C_f := \frac{0.0583}{(\text{Re}_x + 0.001)^{0.2}}$$

These are column vectors each value corresponding to a velocity data point. The addition of 0.001 to the denominator is to prevent a singularity at  $x = 0$ . The Reynolds number is  $\sim 10^5$  and the error in adding 0.001 is totally negligible.

The fit is done to a single sided error function defined by

$$\text{DF}(F) := \begin{cases} 0 & \text{if } F \leq 5 \\ -\text{erf}\left(\frac{-w(F-5)}{2^{0.5}}\right) & \text{otherwise} \end{cases}$$

, with

$$F_{50} = 70$$

$$\sigma_F = \frac{F_{50}}{3}$$

$$w(F) = \frac{F}{\sigma_F}$$

The erf starts at the value 0 at  $F = 5$  and goes to 100% detachment at  $F = 100$ . The actual data is compared to the erf curve and the adjustable parameters are found for the best fit. An example is shown below in Figure 6.

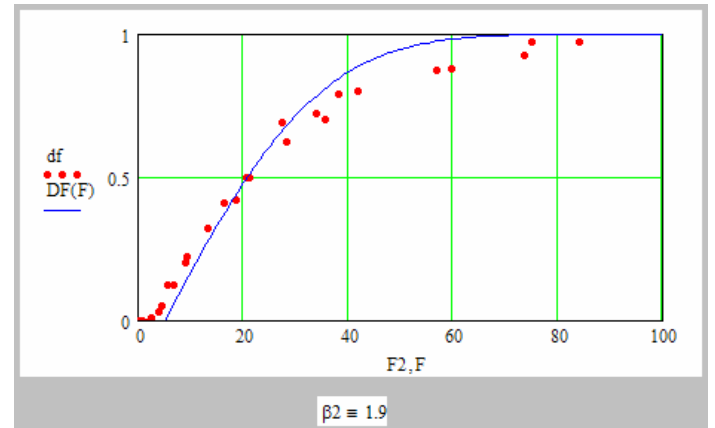


Figure 6. Smooth surface correlation with data on glass microspheres of radius =  $36 \mu$ . With a small area of contact. The scales are from 0 to 100% along df (detachment fraction) axis and from 0 to 100 along F (the rolling moment ratio).

We show an example of data from Iverson et. al. on the behavior of particles at high surface number density in incipient saltation and compare it to a single particle dislodgement in Figure 7.

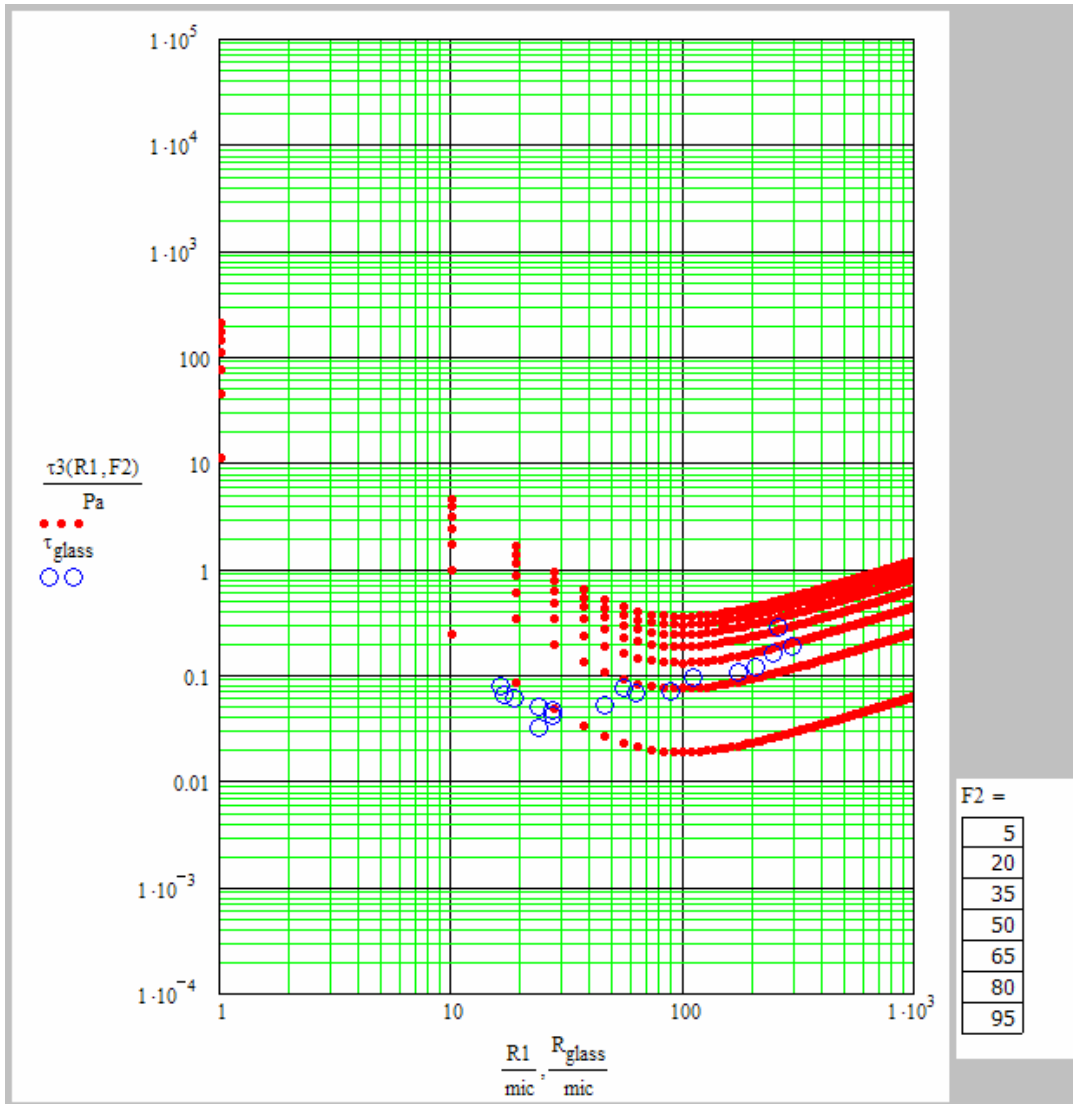


Figure 7. The smooth surface theory plotted in the form of wall shear stress vs. particle size in micron with F as a parameter is compared with data on glass particles. The value  $F = 5$  corresponds to incipient rolling from Essawey's data. Incipient motion data from Iverson is not linked to a specific F because detachment was not measured. Incipient motion appears to cover a range of F from less than 5 with no particle detachment to  $F = 35$  where about 70% detachment would occur for spherical particles. Below the lowest red curve there is no dislodgement and above the highest curve there is nothing left to dislodge. The point of minimum stress is near  $100 \mu$  for glass in earth's gravity.

## PARTICLE DETACHMENT AND TRAJECTORIES

The next steps involve the following. An input spectrum is specified describing the particle number density vs. particle size of the initial contamination on the spacecraft. The total number in each bin

size is distributed at random on various surfaces and subjected to a wind profile described as a series of triplets giving magnitude, direction and duration. The duration could be replaced by an event number because at each event, all particles that can come off do so promptly in a few seconds and nothing

happens afterwards unless the wind increases in magnitude. If the wind increases, more particles come off etc. At each event, the location of the stagnation point, the regions of attached and detached flows (zero wall friction) are located, wall friction at the location of the particle of interest found and the detachment fraction calculated. Both the number that remain and the number that are carried away are determined.

There is a radial flow in the region surrounding a stagnation point. The particle moves along a radial line till it gets to an edge and continues on the surface if the flow is attached. If not it becomes free and travels with the free stream. The side in contact with the wake is in dead air and no particle dislodgement takes place there. The

stagnation points change with wind direction and are found for each wind direction. If the angle between the wind and inward normal is less than 45 deg, the stagnation point is on that surface. If the angle exceeds 45 deg, the stagnation point is on an adjoining face where the above angle is less than 45 deg to its inward normal.

The motion of particles can be seen as a particle path or if only the final landing points are of interest, the final coordinates calculated. The trajectories are almost straight. The surface winds follow the ground and the pattern of particles deposited is similar to the ones deposited on a flat plane. An example of a particle distribution is shown in figure 8 for a wind that rotates from 0 to 180 deg as shown below.

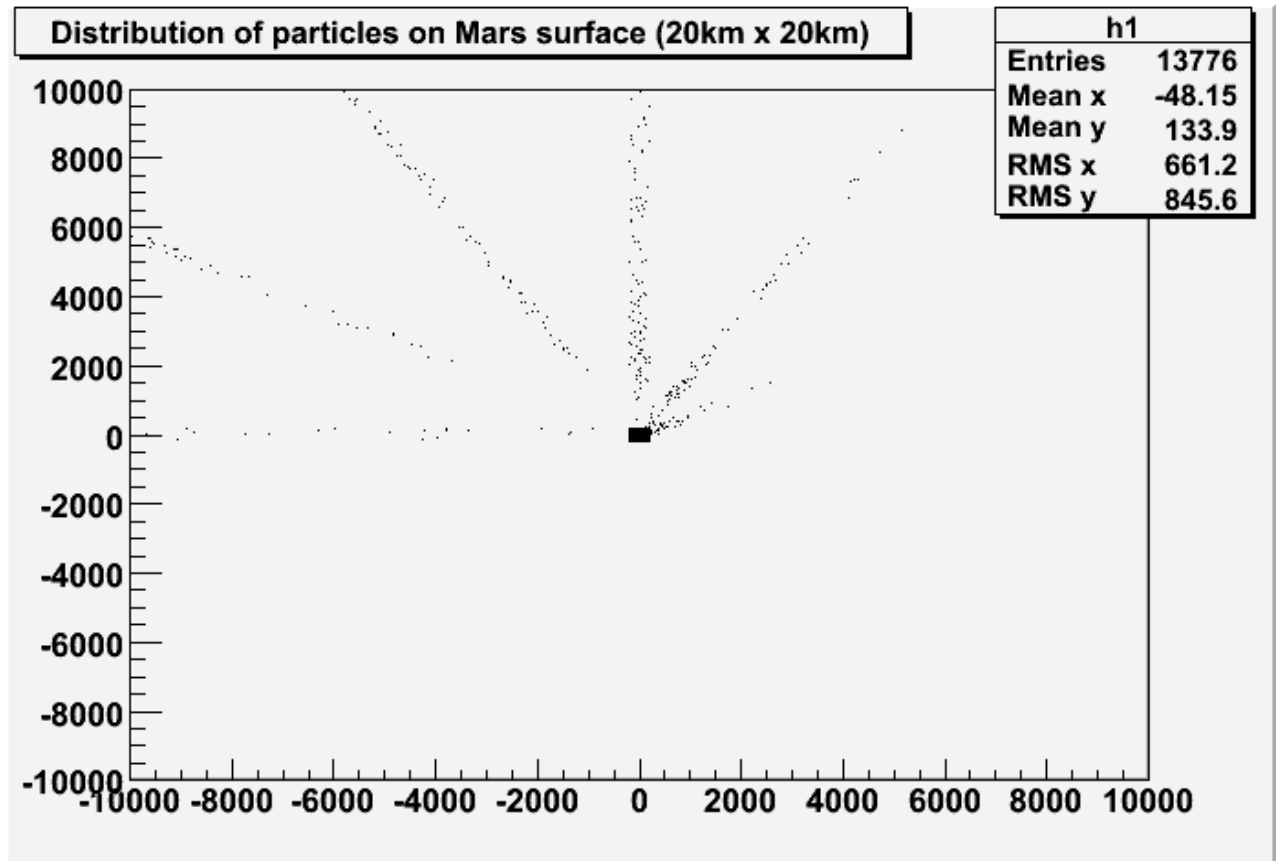


Figure 8. The distribution of particles on the ground is shown. Because the particles fall so slowly, they are carried to large distances from the lander. In this plot particle sizes are not shown with different symbols. The above plot pertains to a full geometry lander described by a vrml file. Each experiment (7 winds) takes 470 secs to

run, for a total of ~50,000 particles. The triplet of numbers refers to event number, magnitude and angle respectively. WIND:(0,1,0) (0.01,5,30) (0.02,9,60) (0.03,13,90) (0.04,17,120) (0.05,21,150) (0.06,25,180) i.e. angle increases with velocity

The research described in this (publication or paper) was carried out at the Jet Propulsion Laboratory, California Institute of Technology, under a contract with the National Aeronautics and Space Administration. Specifically, support for this proposal MT03-0069-0008 called

“Near Field and Integrated Particle Transport Models for Planetary Protection and their Experimental Validation” was provided by NASA Mars Exploration Program, Code SM, Office of space Science.

## REFERENCES

1. Johnson KL, Kendall K, Roberts AD. 1971 . *Proc. R. SOC London Ser. A* 324: 301
2. Derjaguin BV, Muller VM, Toporov Yu. P. 1975. *J. Colloid Interface Sci.*53:314
3. Maugis D, Pollock HM. 1984. *Acta Metall.*32; 1323
4. Rogers LN, Reed J. 1984. *J. Phys. D* 17:677
5. Rimai and DeMejo “Physical Interactions affecting the adhesion of dry particles” , *Annual Rev. Material Sci.* 1996. 26:21-41, also available as *Annual Reviews*, [www.annualreviews.org/aronline](http://www.annualreviews.org/aronline).
6. Johnson KL, Pollock HM. 1994. *J. Adhesion Sci. Technol.* 8: 1323
7. Derjaguin BV. 1934. *Kolloid Z.* 69:155
8. Hamaker HC. 1937. *Physicu* 4:1058
9. Goel NS, Spencer PR. 1975. In *Adhesion Science and Technology*, ed LH Lee pp. 763-827. New York &: Plenum
10. Kendall K, “The adhesion and surface energy of elastic solids”, *J. Phys.*

*D. Appl. Phys.*, Vol 4. Printed in Great Britain.

11 Ibrahim Essawey, “Microparticle detachment from surfaces by fluid flow” by *Abdelmaged Hafez Ibrahim Essawey’s Ph.D thesis, Notre Dame, Indiana, Jan 2004, pp1-139.*, available on the web.

12. Ibrahim A.H, Dunn P.F. and Brach R.F. “Microparticle detachment from surfaces exposed to turbulent air flow; controlled experiments and modeling”, *Aerosol Science* 34 (2003) 765-782, available on the web.

13. Iverson J.D., Pollack J.B. and Greeley R. “Saltation Threshold on Mars: The effect of Interparticle Force, Surface Roughness, and Low Atmospheric Density”, *ICARUS* 29, 381-393 (1976)

14. Phillips M. “A force balance model for particle entrainment into a fluid stream”, *J.Phys, D; Appl Phys.*, 13 (1980) 221-33. Printed in Great Britain

15. Grimes, J. JPL Presentation “ Microparticle Detachment Analysis: Correlation and scaling of Data”, 11 August 2006.

